Rethinking Remdesivir: Synthesis of Lipid Prodrugs that Substantially Enhance Anti-Coronavirus Activity

Robert T. Schooley*,+, Aaron F. Carlin+, James R. Beadle, Nadejda Valiaeva, Xing-Quan Zhang, Aaron F. Garretson, Victoria I. Smith, Joyce Murphy and Karl Y. Hostetler*,#

Division of Infectious Diseases and Global Public Health, Department of Medicine;
University of California San Diego, School of Medicine,
9500 Gilman Drive, La Jolla, California 92093-0676, USA.

Running title: Lipid prodrugs of Remdesivir in SARS-CoV-2 infection

+ These authors contributed equally to the manuscript

***** Corresponding Authors:

Robert T. Schooley
Email: rschooley@health.ucsd.edu

#Karl Y. Hostetler
Email: khostetler@health.ucsd.edu

KEYWORDS: SARS-CoV-2, Remdesivir, Remdesivir nucleoside, antiviral agents, lipid prodrugs, Vero E6 cells

ABSTRACT

The FDA has granted Remdesivir (RDV, GS-5734) an emergency use authorization on the basis of an acceleration of clinical recovery in hospitalized patients with COVID-19. Unfortunately, the drug must be administered intravenously, restricting its use to those with relatively advanced disease. RDV is also unstable in plasma and has a complex activation pathway which may contribute to its highly variable antiviral efficacy in SARS-CoV-2 infected cells. A potent orally bioavailable antiviral for early treatment of SARS-CoV-2 infection is needed. We focused on making simple orally bioavailable lipid analogs of Remdesivir nucleoside (RVn, GS-441524) that are processed to RVn-monophosphate, the precursor of the active RVn-triphosphate, by a single step intracellular cleavage. In addition to likely improved oral bioavailability and simpler metabolic activation, two of the three new lipid prodrugs of RVn had anti-SARS-CoV-2 activity 9 to 24 times greater than that of RDV in Vero E6 cells

INTRODUCTION

Over the past 18 years, spillover events have introduced the highly transmissible beta-coronavirus strains SARS CoV, MERS CoV, SARS CoV-2 into the human population.[1-3] Although case fatality ratios have varied, each has demonstrated the ability to induce substantial morbidity and mortality – especially among those over 55 and/or those with underlying co-morbid medical conditions.[4,5] Although SARS CoV and MERS CoV were largely contained by epidemiological interventions, the current outbreak has evolved into a global pandemic responsible for over 23 million infections and over 800,000 deaths.[6] With over 5.5 million cases and over 175,000 deaths at this writing, the US is now the center of the epidemic. Intensive economically disruptive social distancing measures are blunting the epidemic but they are not sustainable and experience elsewhere demonstrates viral resurgence when they are prematurely eased.[7] Although intensive efforts to develop safe and effective SARS CoV-2 vaccines have been launched using a slew of novel approaches, the effort is challenged by strain diversity, the possibility that vaccine-induced immunity will be short lived, potentially reduced immune recognition by individuals as young as 30 and the possibility that antibody dependent enhancement will be observed.[8,9] Indeed, a recently reported molecularly proven case of reinfection raises substantial new concerns about long-lasting immunity – even after recovery from natural infection. [10] While there is hope that the SARS CoV-2 vaccine effort will succeed, after a third of a century the AIDS vaccine is, alas, still around the corner. Despite admonitions that we “could not treat our way out of the epidemic”, a highly successful drug development effort changed the face of HIV by providing extremely effective, affordable and scalable prevention and

treatment tools. As the coronavirus vaccine effort ramps up, it is essential that we also mount an equally intense therapeutics effort. Remdesivir nucleoside triphosphate (RVn triphosphate) potently inhibits enzymatic activity of the polymerase of every coronavirus tested thus far, including SARS CoV-2. [11-14] This broad activity reflects the

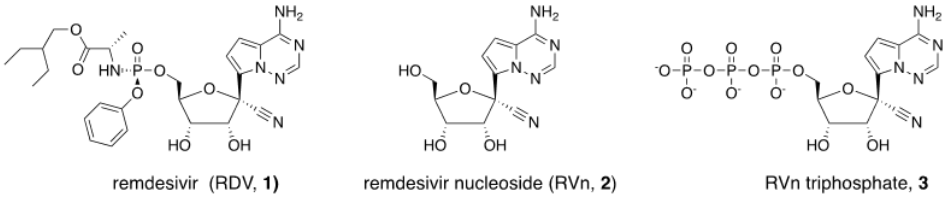

Figure 1. Structures of Remdesivir and related intermediates

relative molecular conservation of the coronavirus RNA dependent RNA polymerase (RdRp). Remdesivir (RDV) is an aryloxy phosphoramidate triester prodrug that must be converted by a series of reactions to RVn triphosphate, the active antiviral metabolite. (Fig 1) Although RVn-triphosphate is an excellent inhibitor of the viral RdRp [15], RDV's antiviral activity is highly variable in different cell types which may be due to variable expression of the four enzymes required for conversion to RVn-P [14]. RDV's base is a 1'-cyano-substituted adenine C nucleoside (GS-441524, RVn) that is thought to be poorly phosphorylated. To bypass the perceived slow first phosphorylation the developers relied on an aryloxy phosphoramidate triester prodrug that is converted by a complex series of four reactions to remdesivir nucleoside monophosphate (RVn-P) that is then efficiently converted to RVn triphosphate, the active metabolite. RDV may be more active in some SARS-CoV-2 infected tissues than in others, a possible reason for its incomplete clinical impact on SARS-CoV-2. A recent report suggests that low levels

of the four enzymes which activate RDV in some tissues may be responsible. [14] Yan and Muller have recently published a detailed analysis of the potential weaknesses of Remdesivir and suggested that RVn (GS-441524) might be a preferable therapy [16]. Remdesivir has beneficial antiviral and clinical effects in animal models of coronavirus infection. [17,18] These effects are primarily demonstrable when administered before or very soon after viral challenge. RDV is not highly bioavailable following oral administration and must be administered intravenously, functionally limiting its clinical application to hospitalized patients with relatively advanced disease. It would be useful to have a highly active, orally bioavailable analog of RVn which provides sustained levels of intact antiviral drug in plasma since RDV persistence in plasma is known to be very short, 20 to 30 minutes. [16]

Here we report the synthesis and antiviral evaluation of three novel lipophilic prodrugs of RVn-monophosphate that are substantially more active than Remdesivir in Vero E6 cells infected with SARS-CoV-2. These compounds are expected to be orally bioavailable based on our prior work with antivirals of this general design. [19, 20] If further developed, this type of prodrug could allow earlier and more effective treatment at the time of diagnosis of SARS-CoV-2 infection. In addition, one of these prodrugs represents an approach that may be able to target the antiviral to the lung and away from the liver, the site of Remdesivir's dose-limiting toxicity. [21,22]

RESULTS

Synthesis of RVn monophosphate prodrugs: We synthesized the hexadecyloxypropyl-, octadecyloxyethyl- and 1-O-octadecyl-2-O-benzyl-sn-glyceryl-esters of RVn monophosphate. Compounds **5a** -**5c** were synthesized as shown in Figure 2. Analyses by NMR, ESI mass spec and HPLC were consistent with each structure and demonstrated purities of > 95%.

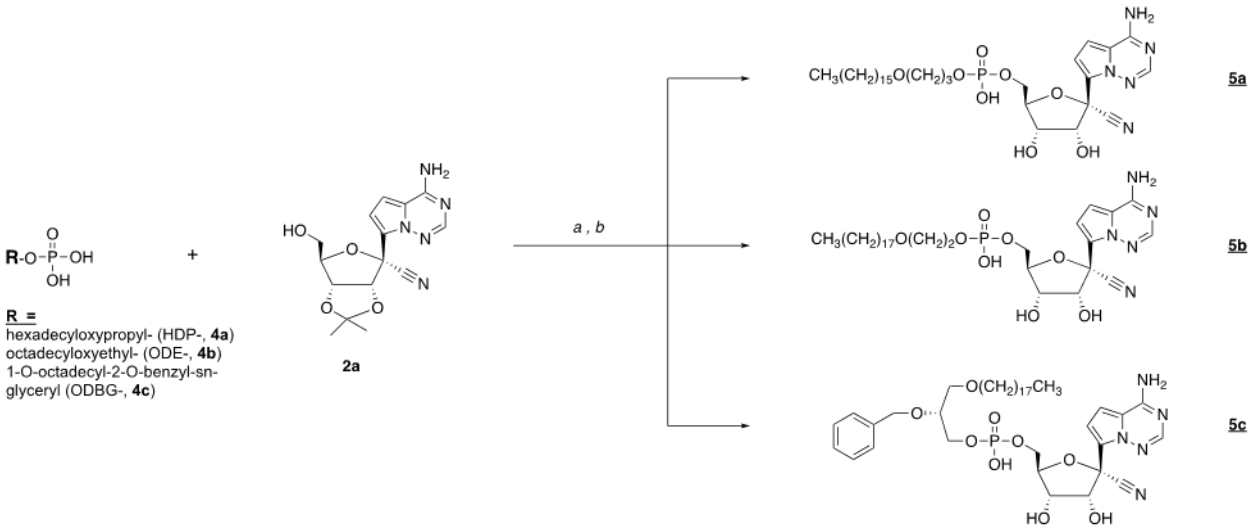

Figure 2. Synthesis of antiviral prodrugs **5a** – **5c**. *Reagents:* a) 2',3'-isopropylidene RVn (**2a**), DCC, DMAP, pyridine, 90 ºC, 24-72 h; b) 37% HCl, THF, 3-18h.

Antiviral Activity: We generated concentration-response curves for ODBG-P-RVn, ODE-P-RVn, and HDP-P-RVn, Remdesivir (RDV) and Remdesivir nucleoside (RVn) for SARS-CoV-2 infection in Vero E6 cells in two separate experiments performed in duplicate (Figure 3).

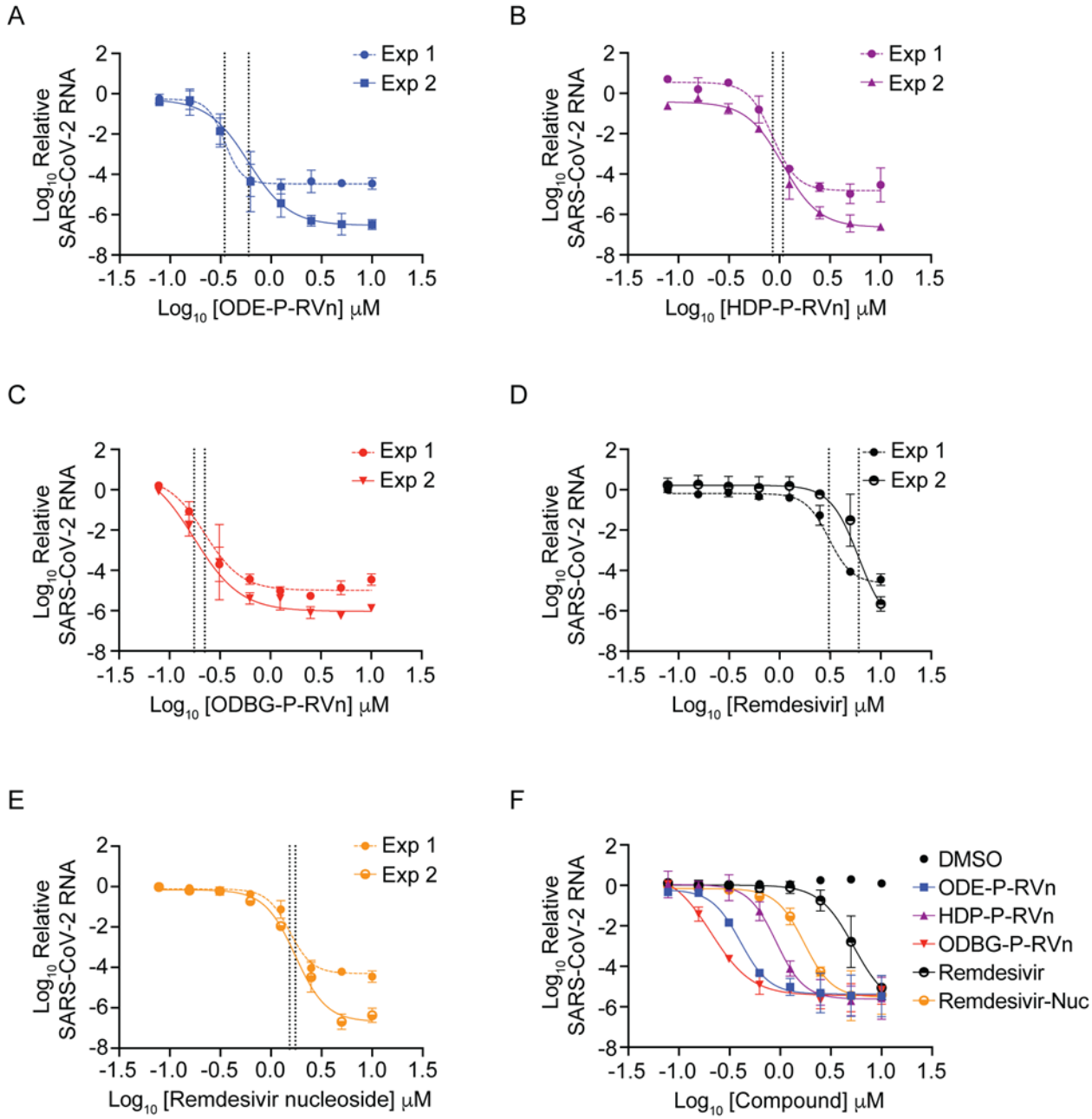

Figure 3. SARS-CoV-2 inhibitory activity replicate experiments. Dose response curves for three Remdesivir analogs, Remdesivir (GS-5734), and Remdesivir nucleoside (GS-441524) against SARS-CoV-2 infection in Vero E6 cells. Vero E6 cells were pretreated with the indicated dose of the indicated drug for thirty minutes and then infected with SARS-CoV-2 isolate USA-WA1/2020 for 48 hours. The relative SARS-CoV-2 Spike RNA expression was determined by qRT-PCR. Each dose-response comparison was conducted simultaneously for all drugs on 2 separate occasions. (A-E) Data from both experiments are shown. Data points indicate the mean relative expression from duplicate wells. Error bars represent the standard deviations (SDs). The black vertical dashed line indicates the concentrations at which there is 50%

inhibition (EC_{50}). (F). Combined inhibition curves for all five compounds and DMSO on a single chart. DMSO, which was the vehicle for all compounds, had no effect on SARS-CoV-2 replication at the concentrations used. The three lipid esters of RVn-monophosphate were all substantially more active than RDV and RVn.

Table 1 shows the effective concentrations (EC_{50}, EC_{90}), 50% cytotoxic concentration (CC_{50}), and selectivity index of the compounds, mean ± SD. Cytotoxicity (CC_{50}) was assessed using Cell Titer Glo (Supplementary Materials, Figure S1). The EC_{50} values of RDV and RVn were 4.6 and 1.7 μM, respectively. The lipid prodrugs were more active with EC_{50}s ranging from 0.19 ± 0.023 to 0.96 ± 0.17. ODBG-P-RVn and ODE-P-RVn

Table 1. Antiviral Activity, Cytotoxicity and Selectivity of the Compounds

Compound	EC_{50} (μM)	EC_{90} (μM)	CC_{50} (μM)	Selectivity	*p* value vs RDV, RVn
Remdesivir	4.6 ± 2.1	8.9 ± 4.9	>100	>21.7	-
Remdesivir nucleoside	1.7 ± 0.13	3.2 ± 0.77	>100	>58.8	-
HDP-P-RVn, 5a	0.96 ± 0.17	2.1 ± 0.78	51	52	0.02, 0.59
ODE-P-RVn, 5b	0.47 ± 0.18	1.1 ± 0.80	>100	>212	0.004, 0.047
ODBG-P-RVn, 5c	0.19 ± 0.023	0.56 ± 0.0002	46	240	<0.001, 0.005

A graph showing the CC_{50} results by Cell Titer Glo is shown in the Supplemental Materials. Abbreviations: RDV, Remdesivir (GS-5734); RVn, Remdesivir nucleoside (GS-441524); HDP-P-, hexadecyloxypropyl-P-; ODE-P-, octadecyloxyethyl-P-; ODBG-P-, 1-O-octadecyl-2-O-benzyl-glycero-3-P-; Selectivity index, CC_{50}/EC_{50}; statistical analysis comparing $LogEC_{50}$ values from separate experiments by one-way ANOVA.

were the most active and selective compounds. Based on the EC_{50} values the most active compound, ODBG-P-RVn, was 24 times more active than RDV and 8.9 times more active than RVn ($p < 0.001$ and 0.005) with a selectivity index of 240.

DISCUSSION

RDV is a prodrug designed to bypass the first phosphorylation of the Remdesivir nucleoside (RVn) which may be rate limiting in the synthesis of RVn-triphosphate, the active metabolite. This occurs by the successive action of carboxyesterases, cathepsin A and phosphoramidases [16,23]. However, this approach does not appear to provide any benefit in Vero E6 cells, a monkey kidney cell line, as shown by Pruijssers et al [24] and by our results showing the antiviral activity of RVn is greater than that of RDV. Other perceived disadvantages of RDV include a lack of oral bioavailability, a difficult synthesis, instability in plasma, inadequate delivery to lung and hepatotoxicity. [14,16] In patients with Covid-19 and in the Syrian hamster model of SARS-CoV-2 disease, in addition to high viral loads in nasal turbinate, trachea and lung, many other tissues are infected with SARS-CoV-2 as the infection proceeds including intestine, heart, liver, spleen, kidney, brain, lymph nodes and vascular endothelium. [25-29] However, RDV antiviral activity appears to vary widely in lung and kidney cell lines with EC_{50} values of 1.65 μM in Vero E6 cells, 0.28 μM in Calu3 2B4, 0.010 μM in human alveolar epithelial cells (HAE), a 165-fold difference. [24] It has been suggested that this may be due to variable amounts of the enzymes which convert RDV to RVn. [14,16] It will be important to evaluate the antiviral activity of RDV, RVn and these 3 novel lipid prodrugs of RVn in cells representing various tissues which are infected by SARS-CoV-2 and must be treated successfully if the infection is to be cleared.

Of all the perceived disadvantages of RDV, we chose to design prodrugs of RVn which could provide oral bioavailability because an effective oral drug would allow for much earlier treatment of persons diagnosed with SARS-CoV-2 infection. As shown in

this report, we accomplished this by constructing liponucleotides of RVn resembling lysophospholipids that are normally absorbed in the GI tract. The RVn liponucleotides are not metabolized rapidly in plasma and gain rapid entry to the cell often exhibiting greatly increased antiviral activity. [30, 31]. In contrast to the activation of RDV which requires four transformations, intracellular kinase bypass with this kind of compound generates the nucleoside monophosphate when the lipid ester moiety is cleaved in a single reaction catalyzed by acid phospholipase C [32, 33] or acid sphingomyelinase (sphingomyelin phosphodiesterase I) (K. Sandhoff and K. Hostetler, unpublished, 2013). One of the compounds, ODBG-P-RVn, is likely to deliver relatively more drug to lung and less to liver as shown previously in lethal mousepox infection. [34,35] Finally, the synthesis of these lipid prodrugs is much simpler than RDV and is readily scalable.

In conclusion, we synthesized three lipid prodrugs of RVn that are substantially more active than RDV or RVn in Vero E6 cells. The two most active compounds ODBG-P-RVn and ODE-P-RVn were 24 and 9.8 times more active than RDV. These compounds are expected to be orally bioavailable, stable in plasma and provide significant exposure and antiviral activity to all tissues infected with SARS-CoV-2.

MATERIALS AND METHODS

Chemistry: All reagents were of commercial quality and used without further purification unless indicated otherwise. Chromatographic purification was done using the flash method with silica gel 60 (EMD Chemicals, Inc., 230–400 mesh). ^{1}H, ^{13}C and ^{31}P nuclear magnetic resonance (NMR) spectra were recorded on either a Varian VX-500 or a Varian HG-400 spectrometer and are reported in units of ppm relative to internal tetramethylsilane at 0.00 ppm. Electrospray ionization mass spectra (ESI-MS) were recorded on a Finnigan LCQDECA mass spectrometer at the small molecule facility in the Department of Chemistry at University of California, San Diego. Purity of the target compounds was characterized by high performance liquid chromatography (HPLC) using a Beckman Coulter System Gold chromatography system. The analytical column was Phenomenex Synergi™ Polar-RP (4.6 × 150 mm) equipped with a SecurityGuard™ protection column. Mobile phase A was 95% water/5% methanol and mobile phase B was 95% methanol/5% water. At a flow rate of 0.8 mL/min, gradient elution was as follows: 10% B (0–3 min.); 10–95% B (3–20 min.); 95% B (20–25 min.); 95% to 10% B (25–34 min.). Compounds were detected by ultraviolet light (UV) absorption at 274 nm. Purity of compounds was also assessed by thin layer chromatography (TLC) using Analtech silica gel-GF (250 µm) plates and the solvent system: $CHCl_3$/MeOH/conc NH_4OH/H_2O (70:30:3:3 v/v). TLC results were visualized with UV light, phospray (Supelco, Bellefonte, PA, USA) and charring at 400 °C.

Compounds: Remdesivir (GS-5734) and Remdesivir nucleoside (GS-441524) were purchased from AA Blocks (San Diego, CA and Mason-Chem (Palo Alto, CA), respectively.

Synthesis of HDP-P-RVn: 5a. ((2*R*,3*S*,4*R*,5*R*)-5-(4-aminopyrrolo[2,1-*f*][1,2,4]triazin-7-yl)-5-cyano-3,4-dihydroxytetrahydrofuran-2-yl)methyl (3-(hexadecyloxy)propyl) hydrogen phosphate.

N,N-Dicyclohexylcarbodiimide (DCC, 619 mg, 3 mmol) was added to a mixture of **2a** (300 mg, 0.91 mmol, prepared as in Warren et al [36], HDP-phosphate (**4a**, 414 mg, 1.10 mmol, prepared as in Kim et al [37], and 4-dimethylaminopyridine (DMAP, 122 mg, 1.0 mmol) in 25 mL of dry pyridine, and then the mixture was heated to 90 ºC and stirred for 24h. Pyridine was then evaporated and the residue was purified by flash column chromatography on silica gel 60. Gradient elution (CH_2Cl_2/methanol 10-20%) afforded 423 mg (67% yield) of 2',3'-isopropylidene derivative of **5a**. ^{1}H NMR (500 MHz, chloroform-*d*) δ 8.42 (s, 1H), 7.98 (s, 1H), 7.70 (s, 2H), 6.22 (d, *J* = 6.0 Hz, 1H), 5.68 (d, *J* = 6.2 Hz, 1H), 5.15 (d, *J* = 1.0 Hz, 1H), 4.70 (dd, *J* = 3.8, 0.9 Hz, 1H), 4.48 – 4.42 (m, 1H), 4.26 (ddd, *J* = 11.2, 8.5, 2.6 Hz, 1H), 4.15 (ddd, *J* = 11.1, 8.5, 2.6 Hz, 1H), 4.02 (dt, *J* = 8.5, 6.3 Hz, 2H), 3.49 (t, *J* = 6.1 Hz, 2H), 3.40 (t, *J* = 6.1 Hz, 2H), 1.95 (p, *J* = 6.2 Hz, 2H), 1.54 (tt, *J* = 7.4, 6.1 Hz, 2H), 1.31 (s, 3H), 1.32 – 1.24 (m, 26H), 0.94 – 0.85 (m, 3H). ESI MS 691.6 $[M-H]^-$.

Concentrated HCl (0.1 mL) in tetrahydrofuran (THF) was added to a stirred solution of 2',3'-isopropylidene-**5a** (100 mg, 0.14 mmol) in THF (10 mL) at room temperature. The mixture was stirred for 3h and then sodium bicarbonate (50 mg) and water (2 mL) were added. After stirring an additional 15 min. the solvents were evaporated and cold water (10 mL) was added to the residue. The solid product was collected by vacuum filtration and dried under vacuum to yield compound **5a** (79 mg, 87% yield) as an off-white solid. ^{1}H NMR (500 MHz, $CDCl_3$-methanol-d_4) δ ppm ^{1}H NMR (500 MHz, Chloroform-*d*) δ

8.42 (s, 1H), 7.98 (s, 1H), 7.70 (s, 1H), 6.22 (d, *J* = 6.0 Hz, 1H), 5.70 (d, *J* = 6.0 Hz, 1H), 5.12 (d, *J* = 4.2 Hz, 1H), 4.55 (ddd, *J* = 5.5, 2.7, 0.9 Hz, 1H), 4.40 (dtd, *J* = 6.8, 2.6, 0.8 Hz, 1H), 4.33 – 4.27 (m, 2H), 4.25 (ddd, *J* = 11.1, 8.4, 2.6 Hz, 1H), 4.16 (ddd, *J* = 11.3, 8.5, 2.6 Hz, 1H), 4.02 (dt, *J* = 8.5, 6.3 Hz, 2H), 3.49 (t, *J* = 6.1 Hz, 2H), 3.40 (t, *J* = 6.1 Hz, 2H), 1.95 (p, *J* = 6.2 Hz, 2H), 1.59 – 1.50 (m, 1H), 1.34 – 1.24 (m, 23H), 0.94 – 0.85 (m, 3H). ESI MS: 652.39 $[M-H]^-$. Purity by HPLC: 99.7%

Synthesis of ODE-P-RVn, 5b. ((2*R*,3*S*,4*R*,5*R*)-5-(4-aminopyrrolo[2,1-*f*][1,2,4]triazin-7-yl)-5-cyano-3,4-dihydroxytetrahydrofuran-2-yl)methyl (2-(octadecyloxy)ethyl) hydrogen phosphate

N,N-Dicyclohexylcarbodiimide (DCC, 0.3 g, 1.4 mmol) was added to a mixture of **2a** (0.23 g, 0.7 mmol), ODE-phosphate (**4b**, 0.27 g, 0.68 mmol), and 4-dimethylaminopyridine (DMAP, 0.07 g, 0.6 mmol) in 10 mL of dry pyridine, and then the mixture was heated to 90 ºC and stirred for 3 days. Pyridine was then evaporated and the residue was purified by flash column chromatography on silica gel 60. Gradient elution (CH_2Cl_2/methanol 10-20%) afforded 0.22 g (45% yield) of 2',3'-isopropylidene-**5b**. Concentrated HCl (0.3 mL) was added slowly to a stirred solution of 2',3'-isopropylidene-**5b** (0.2 g, 0.28 mmol) in tetrahydrofuran (2 mL) at 0 ºC. The mixture was allowed to warm to room temperature overnight and then was diluted with water (2 mL) and adjusted to pH = 8 by adding saturated sodium bicarbonate. The product was extracted with chloroform (3 x 30 mL) and the organic layer was concentrated under reduced pressure. The residue was purified by flash chromatography on silica gel. Elution with 20% MeOH/CH_2Cl_2 gave 0.10 g (55% yield) of compound **5b**. ^{1}H NMR (400 MHz, $CDCl_3$-methanol-d_4) δ ppm 7.89 (s, 1 H), 6.94 (d, *J*=4.65 Hz, 1H), 6.89 (d, *J*=4.65

Hz, 1H), 4.40 (d, *J*=4.65 Hz, 2H), 4.21 - 4.28 (m, 1H), 4.12 - 4.20 (m, 1H), 4.04 - 4.12 (m, 1H), 3.91 (d, *J*=4.89 Hz, 2H), 3.46 - 3.57 (m, 2H), 3.42 (td, *J*=6.85, 1.96 Hz, 2H), 3.34 (dt, *J*=3.18, 1.59 Hz, 2H), 1.53 (d, *J*=6.85 Hz, 2H), 1.20 - 1.37 (m, 30H), 0.89 (t, *J*=6.97 Hz, 3H). ESI MS: 666.43 $[M-H]^-$. Purity by HPLC 98.4%.

Synthesis of ODBG-P-RVn, 5c. ((2*R*,3*S*,4*R*,5*R*)-5-(4-aminopyrrolo[2,1-*f*][1,2,4]triazin-7-yl)-5-cyano-3,4-dihydroxytetrahydrofuran-2-yl)methyl ((*R*)-2-(benzyloxy)-3-(octadecyloxy)propyl) hydrogen phosphate.

N,N-Dicyclohexylcarbodiimide (DCC, 310 mg, 1.5 mmol) was added to a mixture of **2a** (300 mg, 0.91 mmol), ODBG-phosphate (**4c**, 515 mg, 1.0 mmol), and 4-dimethylaminopyridine (DMAP, 122 mg, 1.0 mmol) in 25 mL of dry pyridine, and then the mixture was heated to 90 ºC and stirred for 24h. Pyridine was then evaporated and the residue was purified by flash column chromatography on silica gel 60. Gradient elution (CH_2Cl_2/methanol 10-20%) afforded 210 mg (28% yield) of compound 2',3'-isopropylidene-**5c**. ESI MS 826.58 $[M-H]^-$. Concentrated HCl (0.1 mL) in tetrahydrofuran (THF) was added to a stirred solution of 2',3'-isopropylidene-**5c** (210 mg, 0.25 mmol) in THF(10 mL) at room temperature. The mixture was stirred for 3h and then sodium bicarbonate (50 mg) and water (2 mL) were added. After stirring an additional 15 min. the solvents were evaporated and cold water (10 mL) was added to the residue. The solid product was collected by vacuum filtration and dried under vacuum to yield compound **5c** (71 mg, 36% yield) as an off-white solid. ^{1}H NMR (400 MHz, $CDCl_3$-methanol-d_4) δ ppm 7.70 (s, 1H), 7.36 – 7.32 (m, 1H), 7.36 – 7.26 (m, 1H), 6.22 (d, *J* = 6.0 Hz, 1H), 5.70 (d, *J* = 6.0 Hz, 1H), 5.12 (d, *J* = 4.2 Hz, 1H), 4.60 – 4.51 (m, 2H), 4.40 (dtd, *J* = 6.8, 2.6, 0.8 Hz, 1H), 4.33 – 4.27 (m, 1H), 4.25 (ddd, *J* = 11.0, 8.4, 2.6 Hz, 1H),

4.20 – 4.02 (m, 2H), 3.94 (p, *J* = 4.5 Hz, 1H), 3.59 (d, *J* = 4.4 Hz, 1H), 3.46 (t, *J* = 6.4 Hz, 1H), 1.59 – 1.50 (m, 1H), 1.34 – 1.24 (m, 18H), 0.94 – 0.85 (m, 2H). ESI MS: 786.48 $[M-H]^-$. Purity by HPLC: 97.6%.

Cells: Vero E6 were obtained from ATCC and grown in DMEM (Corning) with 10% FBS and Penicillin-Streptomycin (Gibco).

SARS-CoV-2 infection: SARS-CoV-2 isolate USA-WA1/2020 (BEI Resources) was propagated and infectious units quantified by plaque assay using Vero E6 (ATCC) cells. Approximately 10^4 Vero E6 cells per well were seeded in a 96 well plate and incubated overnight. Compounds or controls were added at the indicated concentrations 30 minutes prior to infection followed by the addition of SARS-CoV-2 at a multiplicity of infection equal to 0.01. After incubation for 48 hours at 37°C and 5% CO_2, cells were washed twice with PBS and lysed in 200ul TRIzol (ThermoFisher).

RNA extraction, cDNA synthesis and qPCR: RNA was purified from TRIzol lysates using Direct-zol RNA Microprep kits (Zymo Research) according to manufacturer recommendations that included DNase treatment. RNA was converted to cDNA using the iScript cDNA synthesis kit (BioRad) and qPCR was performed using iTaq universal SYBR green supermix (BioRad) and an ABI 7300 real-time pcr system. cDNA was amplified using the following primers RPLP0 F – GTGTTCGACAATGGCAGCAT; RPLP0 R – GACACCCTCCAGGAAGCGA; SARS-CoV-2 Spike F – CCTACTAAATTAAATGATCTCTGCTTTACT; SARS-CoV-2 Spike R – CAAGCTATAACGCAGCCTGTA. Relative expression of SARS-CoV-2 Spike RNA was

calculated by delta-delta-Ct by first normalizing to the housekeeping gene RPLP0 and then comparing to SARS-CoV-2 infected Vero E6 cells that were untreated (reference control). Curves were fit and 50 and 90% effective concentrations EC_{50} and EC_{90} values calculated using Prism 8.

CellTiter-glo luminescent cell viability assay: Approximately 10^4 Vero E6 cells per well were seeded in opaque walled 96 well cell culture plates and incubated overnight. Compounds or controls were added at the indicated concentrations. After incubation for 48.5 hours at 37°C and 5% CO_2, an equal volume of CellTiter-Glo reagent (Cat. # G7570, Promega, Madison, WI) was added, mixed and luminescence recorded on an EnSpire Multimode Plate Reader (PerkinElmer) according to manufacturer recommendations. Viability was calculated compared to untreated controls and CC_{50} values were calculated using Prism 8 (Supplemental Materials, Table S1).

ACKNOWLEDGEMENTS

This research was supported by NIAID grant RO1 AI131424, the San Diego Center for AIDS Research and by a Career Award for Medical Scientists from the Burroughs Wellcome Fund to AFC. The following reagent was deposited by the Centers for Disease Control and Prevention and obtained through BEI Resources, NIAID, NIH: SARS-Related Coronavirus 2, Isolate USA-WA1/2020, NR-52281.

REFERENCES

1. Zhong NS, Zheng BJ, Li YM, et al. Epidemiology and cause of severe acute respiratory syndrome (SARS) in Guangdong, People's Republic of China, in February, 2003. Lancet 2003;362:1353-1358.
2. Zaki AM, van Boheemen S, Bestebroer TM, Osterhaus AD, Fouchier RA. Isolation of a novel coronavirus from a man with pneumonia in Saudi Arabia. N Engl J Med 2012;367:1814-1820.
3. Zhu N, Zhang D, Wang W, et. al. China Novel Coronavirus Investigating and Research Team. N Engl J Med. 2020;382:727-733. doi: 10.1056/NEJMoa2001017.
4. Wu C, Chen X, Cai Y, et al. Risk factors associated with acute respiratory distress syndrome and death in patients with coronavirus disease 2019 pneumonia in Wuhan, China. JAMA Intern Med 2020 March 13
5. Zhou F, Yu T, Du R, et al. Clinical course and risk factors for mortality of adult inpatients with COVID-19 in Wuhan, China: a retrospective cohort study. Lancet 2020;395:1054-1062.
6. Center for Systems Science and Engineering of the Johns Hopkins University. https://coronavirus.jhu.edu/map.html (accessed August 13, 2020)
7. To KK, Chan WM, Ip JD, et al. Unique SARS-CoV-2 clusters causing a large COVID-19 outbreak in Hong Kong [published online ahead of print, 2020 Aug 5]. *Clin Infect Dis*. 2020;ciaa1119. doi:10.1093/cid/ciaa1119
8. Graham RL, Donaldson EF and Baric R. A decade after SARS: strategies for controlling emerging coronaviruses. Nat Rev Microbiol 2013; 11: 836-848.
9. Moore JP, Klasse PJ. SARS-CoV-2 vaccines: 'Warp Speed' needs mind melds not warped minds [published online ahead of print, 2020 Jun 26]. *J Virol*. 2020;JVI.01083-20. doi:10.1128/JVI.01083-20
10. To KK, Hung IF, Ip JD, et al. COVID-19 re-infection by a phylogenetically distinct SARS-coronavirus-2 strain confirmed by whole genome sequencing [published online ahead of print, 2020 Aug 25]. *Clin Infect Dis*. 2020;ciaa1275. doi:10.1093/cid/ciaa1275
11. Sheahan TP, Sims AC, Graham RL, et al. Broad-spectrum antiviral GS-5734 inhibits both epidemic and zoonotic coronaviruses. Sci Transl Med 2017; 9:eaal3653-eaal3653.
12. Gordon CJ, Tchesnokov EP, Woolner E, et al. Remdesivir is a direct-acting antiviral that inhibits RNA-dependent RNA polymerase from severe acute respiratory syndrome coronavirus 2 with high potency [published online ahead of print, 2020 Apr 13]. *J Biol Chem*. 2020;jbc.RA120.013679. doi:10.1074/jbc.RA120.013679 Accessed April 20, 2020.
13. Wang M, Cao R, Zhang L, et al. Remdesivir and chloroquine effectively inhibit the recently emerged novel coronavirus (2019-nCoV) in vitro. Cell Res 2020;30:269-271.
14. Yan VC, Muller FL. Advantages of the Parent Nucleoside GS-441524 over Remdesivir for Covid-19 Treatment. *ACS Med Chem Lett*. 2020;11(7):1361-1366. Published 2020 Jun 23. doi:10.1021/acsmedchemlett.0c00316

15. Gordon CJ, Tchesnokov EP, Feng JY, Porter DP, Götte M. The antiviral compound remdesivir potently inhibits RNA-dependent RNA polymerase from Middle East respiratory syndrome coronavirus. J Biol Chem. 2020;295:4773-4779. doi: 10.1074/jbc.AC120.013056. PMCID: PMC7152756.
16. Yan, V., & Muller, F. (2020, August 7). Comprehensive Summary Supporting Clinical Investigation of GS-441524 for Covid-19 Treatment. https://doi.org/10.31219/osf.io/mnhxu
17. de Wit E, Feldmann F, Cronin J, et al. Prophylactic and therapeutic remdesivir (GS-5734) treatment in the rhesus macaque model of MERS-CoV infection. Proc Natl Acad Sci U S A 2020;117:6771-6776.
18. Williamson BN, Feldmann F, Schwarz B, et al. Clinical benefit of remdesivir in rhesus macaques infected with SARS-CoV-2 [published online ahead of print, 2020 Jun 9]. *Nature*. 2020;10.1038/s41586-020-2423-5. doi:10.1038/s41586-020-2423-5
19. Hostetler KY, Beadle JR, Kini GD, Gardner MF, Wright KN, Wu TH, Korba BA. Enhanced oral absorption and antiviral activity of 1-O-octadecyl-sn-glycero-3-phospho-acyclovir and related compounds in hepatitis B virus infection, in vitro. Biochem Pharmacol. 1997 Jun 15;53(12):1815-22. doi: 10.1016/s0006-2952(97)82446-x. PMID: 9256156.
20. Hostetler KY, Beadle JR, Hornbuckle WE, Bellezza CA, Tochkov IA, Cote PJ, Gerin JL, Korba BE, Tennant BC. Antiviral activities of oral 1-O-hexadecylpropanediol-3-phosphoacyclovir and acyclovir in woodchucks with chronic woodchuck hepatitis virus infection. Antimicrob Agents Chemother. 2000 Jul;44(7):1964-9. doi: 10.1128/aac.44.7.1964-1969.2000. PMID: 10858362; PMCID: PMC89993.
21. Buller RM, Owens G, Schriewer J, Melman L, Beadle JR, Hostetler KY. Efficacy of oral active ether lipid analogs of cidofovir in a lethal mousepox model. Virology. 2004 Jan 20;318(2):474-81. PubMed PMID: 14972516.
22. Hostetler KY, Beadle JR, Trahan J, Aldern KA, Owens G, Schriewer J, Melman L, Buller RM. Oral 1-O-octadecyl-2-O-benzyl-sn-glycero-3-cidofovir targets the lung and is effective against a lethal respiratory challenge with ectromelia virus in mice. Antiviral Res. 2007 Mar;73(3):212-8. Epub 2006 Nov 9. PubMed PMID:17123638; PubMed Central PMCID: PMC1859865.
23. Eastman RT, Roth JS, Brimacombe KR, Simeonov A, Shen M, Patnaik S, Hall MD. Remdesivir: A Review of Its Discovery and Development Leading to Emergency Use Authorization for Treatment of COVID-19. ACS Cent Sci. 2020 May 27;6(5):672-683. doi: 10.1021/acscentsci.0c00489. Epub 2020 May 4. Erratum in: ACS Cent Sci. 2020 Jun 24;6(6):1009. PMID: 32483554; PMCID: PMC7202249.
24. Pruijssers AJ, George AS, Schäfer A, Leist SR, Gralinksi LE, Dinnon KH 3rd, et al. Remdesivir Inhibits SARS-CoV-2 in Human Lung Cells and Chimeric SARS-CoV Expressing the SARS-CoV-2 RNA Polymerase in Mice. Cell Rep. 2020 Jul 21;32(3):107940. doi: 10.1016/j.celrep.2020.107940. Epub 2020 Jul 7. PMID: 32668216; PMCID: PMC7340027.
25. Chan JF, Zhang AJ, Yuan S, et al. Simulation of the clinical and pathological manifestations of Coronavirus Disease 2019 (COVID-19) in golden Syrian

hamster model: implications for disease pathogenesis and transmissibility [published online ahead of print, 2020 Mar 26]. Clin Infect Dis. 2020; ciaa325. doi:10.1093/cid/ciaa325

26. Puelles VG, Lütgehetmann M, Lindenmeyer MT, Sperhake JP, Wong MN, Allweiss L, Chilla S, Heinemann A, Wanner N, Liu S, Braun F, Lu S, Pfefferle S, Schröder AS, Edler C, Gross O, Glatzel M, Wichmann D, Wiech T, Kluge S, Pueschel K, Aepfelbacher M, Huber TB. Multiorgan and Renal Tropism of SARS-CoV-2. N Engl J Med. 2020 Aug 6;383(6):590-592. doi: 10.1056/NEJMc2011400. Epub 2020 May 13. PMID: 32402155; PMCID: PMC7240771
27. Ackermann M, Verleden SE, Kuehnel M, Haverich A, Welte T, Laenger F, Vanstapel A, Werlein C, Stark H, Tzankov A, Li WW, Li VW, Mentzer SJ, Jonigk D. Pulmonary Vascular Endothelialitis, Thrombosis, and Angiogenesis in Covid-19. N Engl J Med. 2020 Jul 9;383(2):120-128. doi: 10.1056/NEJMoa2015432. Epub 2020 May 21. PMID: 32437596; PMCID: PMC7412750.
28. Gupta A, Madhavan MV, Sehgal K, Nair N, Mahajan S, Sehrawat TS, Bikdeli B, Ahluwalia N, Ausiello JC, Wan EY, Freedberg DE, Kirtane AJ, Parikh SA, Maurer MS, Nordvig AS, Accili D, Bathon JM, Mohan S, Bauer KA, Leon MB, Krumholz HM, Uriel N, Mehra MR, Elkind MSV, Stone GW, Schwartz A, Ho DD, Bilezikian JP, Landry DW. Extrapulmonary manifestations of COVID-19. Nat Med. 2020 Jul;26(7):1017-1032. doi: 10.1038/s41591-020-0968-3. Epub 2020 Jul 10. PMID: 32651579.
29. Editorial, Progress report on a Pandemic, *Nature* 584, 325 (2020), *doi: 10.1038/d41586-020-02414-1*
30. Hostetler KY. Alkoxyalkyl prodrugs of acyclic nucleoside phosphonates enhance oral antiviral activity and reduce toxicity: current state of the art. Antiviral Res. 2009 May;82(2):A84-98. doi: 10.1016/j.antiviral.2009.01.005. PMID: 19425198; PMCID: PMC2768545.
31. Hostetler KY. Synthesis and early development of hexadecyloxypropylcidofovir: an oral antipoxvirus nucleoside phosphonate. Viruses. 2010 Oct;2(10):2213-25. doi: 10.3390/v2102213. Epub 2010 Sep 30. PMID: 21994617; PMCID: PMC3185567
32. Matsuzawa Y, Hostetler KY. Properties of phospholipase C isolated from rat liver lysosomes. J Biol Chem. 1980 Jan 25;255(2):646-52. PMID: 7356635
33. Hostetler KY, Hall LB. Phospholipase C activity of rat tissues. Biochem Biophys Res Commun. 1980;96:388-93. doi: 10.1016/0006-291x(80)91227-9. PMID: 7437043
34. Kern ER, Collins DJ, Wan WB, Beadle JR, Hostetler KY, Quenelle DC. Oral treatment of murine cytomegalovirus infections with ether lipid esters of cidofovir. Antimicrob Agents Chemother. 2004 Sep;48(9):3516-22. doi: 10.1128/AAC.48.9.3516-3522.2004. PMID: 15328119; PMCID: PMC514741.
35. Hartline CB, Gustin KM, Wan WB, Ciesla SL, Beadle JR, Hostetler KY, Kern ER. Ether lipid-ester prodrugs of acyclic nucleoside phosphonates: activity against adenovirus replication in vitro. J Infect Dis. 2005;191:396-9. Epub 2004 Dec 29. PubMed PMID: 15633099.
36. Warren TK, Jordan R, Lo MK, Ray AS, Mackman RL, Soloveva V, Siegel D, Perron M, Bannister R, Hui HC, Larson N, Strickley R, Wells J, Stuthman KS, Van Tongeren SA, Garza NL, Donnelly G, Shurtleff AC, Retterer CJ, Gharaibeh D, Zamani R, Kenny T, Eaton BP, Grimes E, Welch LS, Gomba L, Wilhelmsen CL, Nichols DK, Nuss JE, Nagle ER, Kugelman JR, Palacios G, Doerffler E,

Neville S, Carra E, Clarke MO, Zhang L, Lew W, Ross B, Wang Q, Chun K, Wolfe L, Babusis D, Park Y, Stray KM, Trancheva I, Feng JY, Barauskas O, Xu Y, Wong P, Braun MR, Flint M, McMullan LK, Chen SS, Fearns R, Swaminathan S, Mayers DL, Spiropoulou CF, Lee WA, Nichol ST, Cihlar T, Bavari S. Therapeutic efficacy of the small molecule GS-5734 against Ebola virus in rhesus monkeys. Nature. 2016 Mar 17;531(7594):381-5. doi: 10.1038/nature17180. Epub 2016 Mar 2. Erratum in: ACS Chem Biol. 2016 May 20;11(5):1463. PMID: 26934220; PMCID: PMC5551389.

37. Kim JS, Beadle JR, Freeman WR, Hostetler KY, Hartmann K, Valiaeva N, Kozak I, Conner L, Trahan J, Aldern KA, Cheng L. A novel cytarabine crystalline lipid prodrug: hexadecyloxypropyl cytarabine 3',5'-cyclic monophosphate for proliferative vitreoretinopathy. Mol Vis. 2012;18:1907-17. Epub 2012 Jul 14. PMID: 22876115; PMCID: PMC3413433.